

Multiphoton detection using visible light photon counter

Jungsang Kim,^{a)} Shigeki Takeuchi,^{b)} and Yoshihisa Yamamoto^{c)}
*ERATO Quantum Fluctuation Project, E. L. Ginzton Laboratory, Stanford University, Stanford,
California 94305*

Henry H. Hogue
Research and Technology Center, Boeing North American, Anaheim, California 92803

(Received 14 September 1998; accepted for publication 8 December 1998)

Visible light photon counters feature noise-free avalanche multiplication and narrow pulse height distribution for single photon detection events. Such a well-defined pulse height distribution for a single photon detection event, combined with the fact that the avalanche multiplication is confined to a small area of the whole detector, opens up the possibility for the simultaneous detection of two photons. In this letter, we investigated this capability using twin photons generated by parametric down conversion, and present a high quantum efficiency ($\sim 47\%$) detection of two photons with good time resolution (~ 2 ns), which can be distinguished from a single-photon incidence with a small bit-error rate ($\sim 0.63\%$). © 1999 American Institute of Physics. [S0003-6951(99)00307-1]

Experimental techniques for single photon detection have made tremendous progress in recent years. High quantum efficiency and low dark counts (background noise) are considered to be the figure-of-merit in characterizing the performance of a single photon detector. Photomultiplier tubes (PMTs) and Si avalanche photodiodes (APDs)¹ have been most widely used, while alternate technologies like solid state photomultipliers (SSPMs),² visible light photon counters (VLPCs),³ and superconducting tunnel junctions (STJs)⁴ have recently demonstrated unique capabilities that PMTs and APDs cannot offer. The quantum efficiency required for detection efficiency loophole free test of Bell inequality (83%) has been realized by the VLPCs ($\sim 88\%$).⁵ STJs offer single photon detection capability with some wavelength resolution (~ 45 nm).⁴ In this letter, we report the capability of VLPCs of detecting two photons. Such capability can be used for the test of Bell inequality,⁶ quantum teleportation experiments⁷ and also for the enhancement of the security in quantum cryptography systems.⁸

Single photon counters should have internal gain mechanism to overcome huge thermal noise generated in the electronic circuits that follow. The noise in this multiplication process determines the distribution of pulse height generated by the single photon detection events.⁹ For the detectors with low multiplication noise, the pulse height originating from a single photon detection event is well defined and there is a possibility to distinguish a single photon detection event from a two photon detection event. PMTs have low noise in the multiplication process,¹⁰ but the single photon quantum efficiency is limited to about $<25\%$ and so the maximum two photon detection efficiency should be only 6%. High quantum efficiency can be achieved by APDs ($\sim 76\%$),¹¹ but the large multiplication noise in these devices completely washes out the correlation between the number of photons

incident and the generated pulse height.^{12,13} In addition to that, for the APDs that operate in Geiger mode for single photon counting, the entire diode breaks down upon detection of a single photon incidence. Therefore, it is impossible to distinguish a two-photon detection event from a single photon detection event.

VLPCs feature noise-free avalanche multiplication and the pulse height resulting from a single photon detection event is very well defined.^{9,14} Furthermore, the avalanche breakdown is confined to a small portion (~ 20 μm diameter) of the total area (1 mm diameter) of the detector. This means that the remainder of the device is still active for another photon detection even if a single photon is detected. These properties open up a possibility for multiple-photon detection using VLPCs. Such behavior has already been observed in previous experiments where the time resolution of the electronic circuit was poor,³ so that more than two photons are detected by the VLPC as a single pulse. In these experiments, however, a difference in the arrival time of the two photons are reflected in the pulse height, which result in significant broadening of the pulse height distribution. Exact quantum efficiency of the two photon detection and the bit-error rate for two photon detection event cannot be determined quantitatively from these experiments.

We have used twin photons generated by a degenerate parametric down-conversion process, where the delay in the arrival times of the two photons can be controlled precisely by optical path length difference.

Figure 1 shows the experimental setup. We used 351.1 nm ultraviolet (UV) radiation from an Ar⁺ laser to pump a BBO crystal in type-II phase-matching configuration. The crystal was slightly tilted away from the colinear phase-matching condition, so that the signal and idler beams (both at 702.2 nm) are completely separated in space.¹⁵ Each of the beams was collimated using a weak focusing lens. One of the beams was delayed, and the two beams were recombined using a polarizing beam splitter. The recombined beam was focused onto the surface of the VLPC through a narrow bandpass filter [centered at 702 nm, and bandwidth of 0.26

^{a)}Electronic mail: jungsang@loki.stanford.edu

^{b)}JST-PRESTO "Field and Reactions", A. T. R. C., Mitsubishi Electric Corporation, Amagasaki, Hyogo 661-8661, Japan.

^{c)}Also affiliated with NTT Basic Research Laboratories, Atsugi, Kanagawa, Japan.

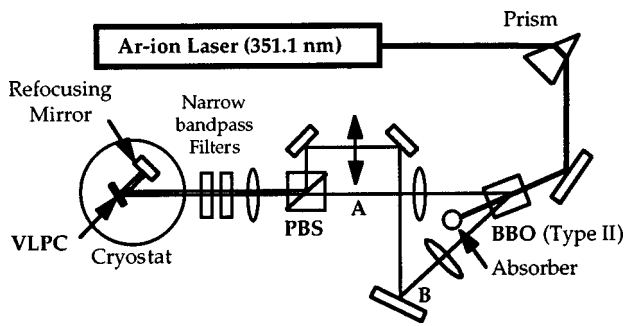


FIG. 1. A schematic of the experimental setup.

nm full-width at half-maximum (FWHM)]. We have installed the VLPC in a bath-type He cryostat where the temperature is stabilized to within 0.005 K using active temperature control. Since the VLPC is extremely sensitive to infrared photons, extensive radiation shields with acrylic windows were used to prevent the room temperature thermal radiation from reaching the detector while keeping transparency at $\sim 97\%$ for 702 nm photons by antireflection coating.⁵ The reflected light from the surface of the detector ($\sim 16\%$) was recollimated using a spherical refocusing mirror and the net reflection loss was reduced to $\sim 2.5\%$. The output signal was amplified by a room temperature preamplifier (MITEQ AUX1347) which has a bandwidth of 500 MHz and provides electrical pulses of 2 ns in width when a single photon is detected.

Figure 2(a) shows an electrical pulse resulting from a single photon detection event. The width of the pulse (2 ns) does not decrease even when the bandwidth of the amplifier is increased, indicating that it is limited by the capacitance of the VLPC (~ 14 pF) and the input impedance of the amplifier (50Ω). Figures 2(b) and 2(c) show the cases when the optical delay between the two beams is 5 and 3 ns, respectively. The heights of the pulses are almost identical, indicating that the number of electrons released per single photon detection event is well defined. Finally, Fig. 2(d) shows when the optical delay is reduced to zero. The two pulses resulting from the two photon detection events completely overlap in time, and the pulse height is twice that of a single photon detection event.

Pulse height analysis can be performed to estimate the bit-error rate for the two-photon detection event. Figure 3 shows the pulse height analysis of the cases when only one of the beams is incident [Fig. 3(a)], and when both beams are incident on the VLPC [Fig. 3(b)]. For the two-beam incidence case, there is a second peak in the pulse height distribution, centered at twice the value (~ 74 mV) of the center of the first peak (~ 37 mV). The theoretical expression for the pulse height distribution for the VLPC is given by the gamma distribution⁹

$$P(M) = \frac{1}{M} \left(\frac{1}{F-1} \frac{M}{\langle M \rangle} \right)^{1/(F-1)} \frac{\exp\left(-\frac{1}{F-1} \frac{M}{\langle M \rangle}\right)}{\Gamma\left(\frac{1}{F-1}\right)}, \quad (1)$$

where M is the statistical variable that describes the multiplication gain, $\langle M \rangle$ is the average of M , and $F = \langle M^2 \rangle / \langle M \rangle^2$ is

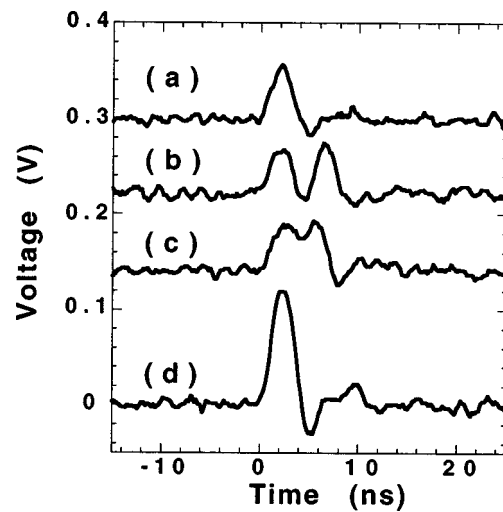


FIG. 2. Real-time trace of photon detection signal recorded by a 5 GS/s digitizing oscilloscope. The time delay between the two beams is changed by modifying the optical path length. The traces are shifted vertically for clarity. (a) Single-photon detection signal. (b) 5 ns delay. (c) 3 ns delay. (d) Zero delay.

the excess noise factor (ENF) for the multiplication process. From the pulse height distribution obtained in the experiment, we can calculate the mean ($\langle M \rangle$) and ENF (F) of the gain, and use these values in Eq. (1) to generate the dotted lines of Fig. 3. For Fig. 3(b), the mean two curves were generated separately to fit each peak, which were then added to give the dotted line shown. The excess noise factor deduced from these pulse height distribution was 1.026 for the single-photon pulse height distribution [in both Figs. 3(a) and 3(b)] and 1.012 for two-photon pulse height distribution, indicating almost noise-free avalanche multiplication. The bit-error rate P_e for distinguishing a two-photon detection event from a single-photon detection event is given by

$$P_e = \min \left\{ \int_{V_T}^{\infty} P_1(V) dV + \int_{-\infty}^{V_T} P_2(V) dV \right\}, \quad (2)$$

where $P_1(V)$ and $P_2(V)$ are the normalized pulse height distribution for single-photon detection events and two-photon detection events, respectively, and V_T is the threshold voltage used for the discrimination. From the two distributions given in Fig. 3(b), P_e is minimized to 0.63% when V_T is chosen at ~ 54 mV. It should be noted that the discriminator level V_T for two-photon detection and the bit-error rate P_e can change slightly depending on the relative size of the two peaks in Fig. 3(b).

The narrow bandpass filter used in front of the VLPC had transmittance of about 50% at 702 nm, and such one photon optical loss is responsible for the small two-photon detection peak compared to the single-photon detection peak. The net quantum efficiency for two-photon detection can be estimated if such optical loss is subtracted. We used two single photon counting modules [(SPCMs); single photon counting detectors based on avalanche photodiodes] to characterize the optical loss and the quality of the two-photon source. Large area ($500 \mu\text{m}$ diameter) APDs are employed in our SPCMs, and the quantum efficiency of these detectors are $\sim 50 \pm 5\%$ near the measurement wavelength of 702 nm.

We placed two SPCMs at locations A and B indicated in Fig.

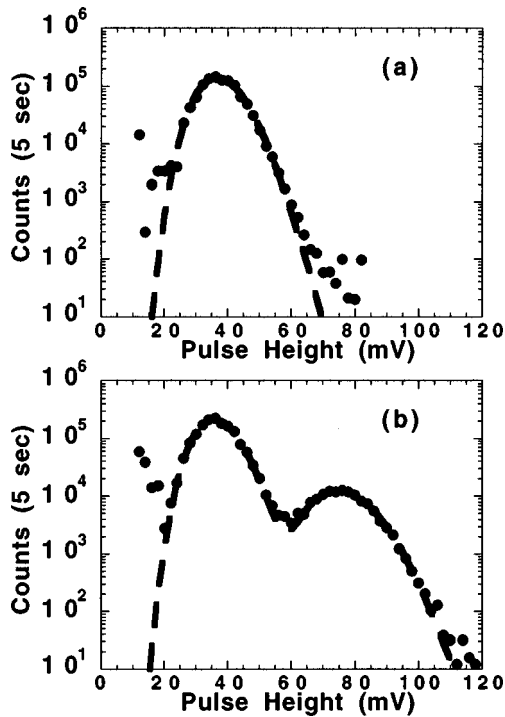


FIG. 3. Pulse height distribution for the detected photons. Counts were integrated for 5 s at each point. The dark circles are experimental data, and the dotted lines are theoretical fits using Eq. (1). (a) Single beam input. (b) Two beam input with zero time delay between the two beams.

1 with narrow bandpass filters in front of each detector and measured the single photon count rates of two beams [A and B , in units of counts per second (cps)] independently, and the coincidence count rate of the two beams (C). Given the dark counts of the SPCMs (which is measured by blocking the input beams) and the quantum efficiency, we can estimate the net photon flux at the SPCM inputs (A_0 and B_0) and the net coincidence input (C_0) (Table I). These three numbers characterize the one photon loss rate of the two-photon source made up of a parametric down converter and all the optical components used, including the narrow bandpass filters.

Once these properties are known, we can estimate the two-photon detection efficiency of the VLPC. The ratio of the two-photon detection events and single-photon detection events is given by

$$\frac{R_2}{R_1} = \frac{\eta_2 C_0}{\eta_1 (A_0 + B_0 - 2\eta_1 C_0) + D_0}, \quad (3)$$

where R_1 and R_2 denote the single- and two-photon count rates, η_1 and η_2 denote the single- and two-photon detection quantum efficiency, and D_0 denotes the dark count rate of the VLPC. Independent measurements at the same operating conditions yield the values $\eta_1 = 70 \pm 5\%$ and $D_0 = 1.7 \times 10^4$ cps for the single-photon detection quantum efficiency and the dark count rate, respectively. Single-photon detection quantum efficiency η_1 was degraded by about 5% because of saturation effect caused by a relatively large input photon flux ($\sim 5.6 \times 10^5$ cps) used in the experiment.⁵ The experi-

TABLE I. Count rates, dark count rates, and coincidence count rates for the two-photon source using SPCM detectors. All numbers are given in units of counts per second (cps).

Quantity	Measured counts	Dark counts	Net counts
A	1.22×10^5	2.59×10^3	2.38×10^5 (A_0)
B	8.41×10^4	1.37×10^4	1.41×10^5 (B_0)
C	1.13×10^4	negligible	4.53×10^4 (C_0)

mental value for R_2/R_1 can be found from integrating the pulse height distribution curve in Fig. 3(b), and is found to be 8.5×10^{-2} . Using these data with the values for A_0 , B_0 , and C_0 in Table I, we can deduce the two-photon detection quantum efficiency $\eta_2 = 47\%$. The maximum value expected for a two-photon detection quantum efficiency is given by $\eta_{2,\max} = \eta_1^2 = 49\%$, and the two-photon detection quantum efficiency in our setup is limited by the single-photon detection quantum efficiency within the measurement accuracy.

In conclusion, we report here a photon detector based on VLPC that can distinguish between a single-photon incidence and two-photon incidence with high quantum efficiency (47%), good time resolution (2 ns), and low bit-error rate ($\sim 0.63\%$). The performance of the detector was tested quantitatively using a two-photon source employing twin photons generated by a degenerate parametric down-conversion process.

J. Kim wants to thank Dr. S. Machida of NTT Basic Research Labs for helpful discussion on the electronic circuits. This work was partly supported by JSEP.

- ¹H. Dautet, P. Deschamps, B. Dion, A. D. MacGregor, D. MacSween, R. J. McIntyre, C. Trotter, and P. P. Webb, *Appl. Opt.* **32**, 3894 (1993).
- ²M. D. Petroff, M. G. Stapelbroek, and W. A. Kleinmans, *Appl. Phys. Lett.* **51**, 406 (1987).
- ³M. Atac, J. Park, D. Cline, D. Chrisman, M. Petroff, and E. Anderson, *Nucl. Instrum. Methods Phys. Res. A* **314**, 56 (1992).
- ⁴A. Peacock, P. Verhoeve, N. Rando, A. van Dordrecht, B. G. Taylor, C. Erd, M. A. C. Perryman, R. Venn, J. Howlett, D. J. Goldie, J. Lumley, and M. Wallis, *Nature (London)* **381**, 135 (1996).
- ⁵S. Takeuchi, J. Kim, Y. Yamamoto, and H. H. Hogue, *Appl. Phys. Lett.* (to be published).
- ⁶P. G. Kwiat, *Phys. Rev. A* **52**, 3380 (1995).
- ⁷S. L. Braunstein and H. J. Kimble, *Nature (London)* **394**, 840 (1998); D. Bouwmeester, J.-W. Pan, M. Daniell, H. Weinfurter, M. Zukowski, and A. Zeilinger, *ibid.* **394**, 841 (1998).
- ⁸T. P. Spiller, *Proc. IEEE* **84**, 1719 (1996).
- ⁹G. B. Turner, M. G. Stapelbroek, M. D. Petroff, E. W. Atkins, and H. H. Hogue, in *SciFi 93-Workshop on Scintillating Fiber Detectors*, edited by A. D. Bross, R. C. Ruchti, and M. R. Wayne (World Scientific, New Jersey, 1993), p. 613; M. G. Stapelbroek and M. D. Petroff, *SciFi 93-Workshop on Scintillating Fiber Detectors* (World Scientific, New Jersey, 1993), p. 621.
- ¹⁰R. S. Bondurant, P. Kumar, J. H. Shapiro, and M. M. Salour, *Opt. Lett.* **7**, 529 (1982).
- ¹¹P. G. Kwiat, A. M. Steinberg, R. Y. Chiao, P. H. Eberhard, and M. D. Petroff, *Phys. Rev. A* **48**, R867 (1993).
- ¹²N. G. Woodard, E. G. Hufstedler, and G. P. Lafyatis, *Appl. Phys. Lett.* **64**, 1177 (1994).
- ¹³R. J. McIntyre, *IEEE Trans. Electron Devices* **ED-13**, 164 (1966).
- ¹⁴J. Kim, Y. Yamamoto, and H. H. Hogue, *Appl. Phys. Lett.* **70**, 2852 (1997).
- ¹⁵S. Takeuchi, *Meeting Abstracts of the Phys. Soc. of Japan* **53**, 292 (1998).